

3B Containment Hydrodynamic Loads

The information in this appendix of the reference ABWR DCD, including all subsections, tables, and figures, is incorporated by reference with the following departures.

STD DEP T1 2.4-3

STD DEP 3B-1

STD DEP 3B-2 (Table 3B-1, Figures 3B-12 and 3B-13)

STD DEP Admin (Figures , 3B-21, 3B-24, 3B-26)

As required by Section IV.A.3 of Appendix A to Part 52 of the ABWR Design Certification Rule, the plant-specific DCD must physically include the proprietary and safeguards information referenced in the ABWR DCD. Appendix 3B in the reference ABWR DCD references proprietary information in tables and figures. That proprietary information is provided in COLA Part 10. It has finality in accordance with Section VI.B.2 of the ABWR Design Certification Rule, and does not constitute a supplement to or departure from the reference ABWR DCD. Tables 3B-2, 3, 4, 5, 6, 7, 8, 9 and Figures 3B-2, 3, 8, 9, 10, 14, 15, 16, 17, 18, 19, 20, 22, 23, 24, 25, 27, 29, 31, 32, 33, and 34 are provided in COLA Part 10 and are unaffected by the departures in this Appendix.

3B.2.2.3 Small Break Accident (SBA)

STD DEP Admin

The SBA is defined as an event in which the fluid loss from the RPV is insufficient to either depressurize the reactor or result in a decrease of reactor water level. Following the break, the drywell pressure will slowly increase until the high drywell pressure scram setting is reached. The reactor will scram, but the MSIVs ~~do not close immediately~~ remain open, and close when reactor water level decreases to RPV Level 1.5.

As a result of a postulated MSIV closure, the SRVs will initially discharge to control reactor vessel pressure in response to the isolation transient. Following the initial SRV discharge, SRV cycling will occur at the SRV setpoint pressure. When the temperature of the suppression pool reaches the Technical Specification limit of ~~54°C~~ 48.9°C during normal operation, the operator will take action to begin a controlled depressurization of the reactor vessel, using manual operation of the SRVs if the MSIVs are closed, or using the main condenser if the MSIVs are open. The rate of depressurization, and thus the total duration of the SBA event, is dependent on operator action. A conservative value for analysis is taken as 56°C/h.

3B.3.3 Quencher Condensation Performance

STD DEP Admin

Recent studies, subsequent to the issuance of NUREG-0783, conclude that steady steam flow through quencher devices (like the X-quencher) is expected to be a stable and smooth condensation process over the full range of pool temperature up to saturation. It is also concluded that the condensation loads ~~for steam discharge from X-quencher~~ are less than the loads from equivalent straight pipes. Figure 3B-8 shows typical pressure amplitudes due to condensation of steam from X-quenchers. These recent studies are described and discussed in Reference 3B-5.

3B.4.2.1 Pool Boundary Loads

STD DEP 3B-2

ABWR Pool Swell Loads

ABWR pool swell response calculations to quantify pool swell loads were based on a simplified, one dimensional analytical model. The model was qualified against test data from the Pressure Suppression Test Facility (PSTF) for a 1/3- scaled Mark III pressure suppression system geometry. The methodology is similar to, ~~same as that reviewed and accepted by the staff (NEDE-21544P/NUREG-0808) for application to Mark II plants. This analytical model was qualified against Mark II full scale test data.~~ The ABWR pressure suppression system design is similar to the Mark III design. The main difference is the smaller gas space above the suppression pool in the ABWR. This difference is accounted for in the analytical model for the pressure suppression system. ~~utilizes a confined wetwell airspace similar to that in Mark II design, but its vent system design is quite different than that in Mark II design. The ABWR vent system design utilizes horizontal vents similar to that in Mark III design. Therefore, recognizing this difference in vent system design, additional studies comparing model against Mark III horizontal vent test data were performed to assure adequacy of the model for application to ABWR.~~

Model Vs. Mark III Horizontal Vent Test Data

Test data used to qualify the analytic model was taken from 1/3-scale tests for a Mark III geometry. The submergence to pool width ratio was representative of conditions in an ABWR. The GOTHIC code was used to model the Mark III tests. The model was designed to bound the test data. The test data used in the model comparison, and the modeling approach, are fully described in Reference 3B-17. ~~Model input/assumptions used in predicting Mark III test data for model comparison were the same as prescribed in NEDE 21544P. Mark III horizontal vent system features were modeled in the following manner:~~ The major modeling assumptions were:

- *~~Pool swell water slug was approximated by a consistent thickness equal to top vent submergence~~*
- The wetwell is represented by a subdivided one-dimensional model

- ~~The Drywell drywell pressure transient and vent clearing times was specified using data from the tests input based on test data~~
- ~~Pressure losses between the measured pressure in the drywell and the weir wall region were ignored to maximize the air flow into the suppression pool~~
- ~~Vent flow area increased in order with the clearing of middle and bottom vents A single horizontal vent, having the full combined open area of the three horizontal vents, was modeled at the elevation of the top vent~~

~~Test data used for model comparison were taken from full scale and sub scale tests, and they were representative of ABWR submergence to pool width ratio. The test data used in model comparison are listed in Table 3B-8.~~

~~Comparison results, summarized in Reference 3B-17 Table 3B-9 and sample results shown graphically in Figures 3B-9 and 3B-10, demonstrate that the model over-predicts the horizontal vent test data. These comparison results demonstrate and assure adequacy of the model for calculating ABWR pool swell response.~~

Pool Swell Loads

~~Pool swell response calculations were done using the same modeling approach and assumptions that were used in the qualification against the 1/3 scale Mark III test data. The model is fully described in Reference 3B-17 analytical model described above. Reference 3B-14 provides a detailed description of the model. The modeling scheme for calculations was consistent with that used for model vs. test data comparison. For an added conservatism in model predictions, water slug surface area occupied by the air bubble was taken as 80% of the total pool surface area in pool swell response calculations.~~

~~The model includes In modeling and simulating the pool swell phenomenon, the following assumptions were made:~~

- (1) ~~Noncondensable gases are assumed to behave as an ideal gas.~~
- (2) ~~After the vent clearing, only noncondensable gases flow through the vent system.~~
- (3) ~~The flow rate of noncondensable gases through the vent system is calculated assuming one-dimensional flow under adiabatic conditions and considering the pipe friction effects with possible choking at the vent exit.~~
- (4) ~~All three horizontal vents are combined into a single flow path that has the total flow area of all 3 vents. The bottom of the single modeled vent is located at the physical bottom of the top vent in the vertical vent pipe. ~~The noncondensable gases contained initially in the drywell are compressed isentropically.~~~~

- (5) The temperature of bubbles is forced to near thermal equilibrium with the pool. (noncondensable gas) in the pool is taken to be the same as that of the noncondensable gases in the drywell (from (4)).
- (6) After the vent clearing, pool water of constant thickness above the top horizontal vent outlet is accelerated upward. The built-in interfacial drag models in GOTHIC are used to predict the bubble expansion and the acceleration of the water above the vents, including differential velocity in the air and water phases resulting in thinning of the slug as it rises.
- (7) Friction between the pool water and the pool boundary and fluid viscosity are is neglected.
- (8) Noncondensable gases present in the wetwell airspace are assumed is compressed by the rising water. For predicting the maximum slug velocity, the air space is assumed to be in thermal equilibrium with the pool to minimize the air space pressure. For predicting the maximum bubble and air space pressure, the air space is assumed to be thermally isolated from the pool. to undergo a polytropic compression process during the pool swell phase.
- (9) Heat transfer to the pool and air space boundaries is ignored. For conservative estimates, a polytropic index of 1.2 will be used for computing the pool swell height and pool swell velocity, and an index of 1.4 for computing pressurization of the wetwell airspace.
- (10) For added conservatism, pool swell velocity obtained in (9) above will be multiplied uniformly by a factor of 1.1 in defining impact/drag loads. The air bubble is constrained to rise in an area that is 80% of the full pool area.

Structures located between 0 and ~~7m~~8.8m above the initial surface will be subjected to impact load by an intact water ligament, where the ~~7m~~8.8m value corresponds to the calculated maximum pool swell height. The load calculation methodology will be based on that approved for Mark II and Mark III containments (NUREG-0487 and NUREG-0978).

Structures located at elevations between the ~~7m~~8.8m and ~~40.3m~~12.1m will be subjected to froth impact loading. This is based on the assumption that bubble breakthrough (i.e., where the air bubbles penetrate the rising pool surface) occurs at ~~7m~~8.8m height, and the resulting froth swells to a height of 3.3m. ~~This froth swell height is the same as that defined for Mark III containment design and this.~~ This is considered to be conservative for the ABWR design. Because of substantially smaller wetwell gas space volume (about 1/5th of the Mark III design), the ABWR containment is expected to experience a froth swell height substantially lower than the Mark III design. The wetwell gas space is compressed by the rising liquid slug during pool swell, and the resulting increase in the wetwell gas space pressure will decelerate the liquid slug before the bubble break-through process begins. The load calculation methodology will be based on that approved for the Mark III containment (NUREG-0978).

As shown in Figure 3B-13 the gas space above the ~~40.3 m~~12.1m elevation will be exposed to spray condition ~~including~~ which is expected to induce no significant loads on structures in that region.

As drywell air flow through the horizontal vent system decreases and the air/water suppression pool mixture experiences gravity-induced phase separation, pool upward movement stops and the "fallback" process starts. During this process, structures between the bottom vent and the ~~40.3 m~~12.1m elevation can experience loads as the mixture of air and water fall past the structure. The load calculation methodology for ~~the~~ defining such loads will be based on that approved for Mark III containment (NUREG-0978).

3B.4.2.3 Impact and Drag Loads

STD DEP 3B-1

STD DEP Admin

As the pool level rises during pool swell, structures or components located above the initial pool surface (but lower than its maximum elevation) will be subjected to water impact and drag loads. The following equations will be used to compute the applicable impact and drag loads on affected structures.

Impact Load

Flat Target:

$$T = (0.011 \times W) / V \text{ for } V \geq 2.13 \text{ m/s}$$

$$= (0.0016 \times W) \text{ for } V < 2.13 \text{ m/s}$$

The equation above is replaced with the following equation below:

$$T = (0.011 \times W) / V \text{ for } V \geq 2.13 \text{ m/s}$$

$$= (0.0052 \times W) \text{ for } V < 2.13 \text{ m/s}$$

where

$$T = \text{Pulse duration, s}$$

$$D = \text{Diameter of cylindrical pipe, m}$$

$$W = \text{Width of the flat structure, m}$$

$$V = \text{Impact velocity, m/s}$$

3B.4.3.2.1 Description of CO Database

STD DEP Admin

A detailed description, evaluation, and discussion of CO data are given in Reference 3B-7.

The test program consisted of a total of 13 simulated blowdowns in sub-scaled test facility representing a one-cell (~~360°~~ 36°) sector of the ABWR horizontal vent design, which included a ~~single~~ single vertical/horizontal vent module. The subscaled (SS) test facility was geometrically (all liner dimensions scaled by a factor of 2.5) similar to the prototypical ABWR design, and the single vertical/horizontal vent module included all three horizontal vents, as shown in Figure 3B-15. In these tests, full-scale thermodynamic conditions were employed. This approach is based on the belief that condensation phenomena at the vent exit are mainly governed by the thermodynamic properties of the liquid and vapor phases. In accordance with this scaling procedure, measured pressure amplitudes are equal to full-scale values at geometrically similar locations, whereas measured frequencies are 2.5 times higher than the corresponding full-scale frequencies. The technical basis for using this scaling approach was based on extensive review and evaluation of the available literature on CO scaling and scaled tests performed for Mark II and Mark III containments, as well as general consensus of technical experts in this field. The CO scaling studies, which have been performed independently by various technical experts, show that for tests in a geometrically scaled facility with full-scale thermodynamic conditions, the measured pressure amplitudes are the same as full-scale values at geometrically similar locations, and measured pressure frequencies are the scale factor times higher than the corresponding full-scale frequencies.

3B.4.3.3.3 Loads on Horizontal Vent

STD DEP Admin

For structure evaluation of the horizontal vent pipe and pedestal, an upward load, based on the HVT test data, is conservatively defined as shown in Figure ~~3B-27~~ 3B-33.

For building structure response analysis for the evaluation of RPV and its internals, the horizontal vent upward load is specified as shown in Figure ~~3B-28~~ 3B-34. To bound symmetrical and asymmetrical loading conditions, the following two load cases will be considered and analyzed.

3B.4.4.1 Exhaust Steam Condensation Loading

STD DEP T1 2.4-3

The RCIC system is a safety system, consisting of a steam turbine, pump, piping, accessories, and necessary instrumentation. ~~The steam turbine exhaust steam piping is ASME Code Class 2 piping, as noted in the RCIC P&ID in Tier 2 Figure 5.4.8.~~

To minimize exhaust steam line vibration and noise levels, the discharge end of the turbine exhaust line will be equipped with a condensing sparger. The sparger design configuration will be similar to that currently used successfully for the operating BWRs. The turbine exhaust piping, including the RCIC sparger, are designed to retain piping pressure integrity and functional capability.

The condensing sparger is expected to produce a very smooth steam condensation operation resulting in low pressure fluctuations in the ~~pool~~ pool, which would imply low

pressure on the pool boundary. ~~During RCIC operation, steam mass flux in the neighborhood of 470.72 Pa/s are expected, which should assure smooth steam condensation process. During the extended RCIC operation, condensing exhaust steam will bring the pool to high temperature. At high pool temperatures, long plumes consisting of a random two-phase mixture of entrained water and steam bubbles are expected to exist. As reported in Reference 3B-16, this plume would not shed large coherent bubbles. Large coherent bubbles are a concern because they may drift and collapse in a cooler region of the pool, the condensation of the steam within such a mixture will not give rise to large bubbles that drift in to a cooler region of the pool and suddenly collapse which could transmit~~ potentially producing significant loads to the pool boundary.

3B.5 Submerged Structure Loads

STD DEP Admin

During SRV actuations, the dynamic process of the steam blowdown is quite similar to LOCA steam blowdown but the induced load is mitigated by the X-quencher device attached at the end of each discharge ~~device line~~. Two types of loads are important. One is due to the water jet formed at the confluence of the X-Quencher ~~arm~~ arms discharges and another is due to the four air bubbles formed between the arms of the X-Quencher. These air bubbles are smaller in size than the LOCA air bubbles, reside longer in the pool, and oscillate as they rise to the free surface of the pool.

3B.7 References

STD DEP Admin

STD DEP 3B-2

3B-13 ~~T. H. Chuang, L. C. Chow, and L. E. Lasher, "Analytical Model for Estimating Drag Forces on Rigid Submerged Structures Caused by LOCA and Safety Relief Valve Ramshead Air Discharges", Supplement for X-Quencher Air Discharge." NEDO-21471, Supplement 1, June 1978. October 1979.~~

3B-17 "Post LOCA Suppression Pool Swell Analysis for ABWR Containment Design," UTLR-0005, Toshiba Corporation, September 2009.

Table 3B-1 Pool Swell Calculated Values

Description	Value
1. Air bubble pressure (maximum)	133.37 kPaG 195 kPaG
2. Pool swell velocity (maximum)	10.9 m/s
3. Wetwell airspace pressur (maximum)	107.87 kPaG 146 kPaG
4. Pool swell height (maximum)	7m 8.8m

Figure 3B-11 Pool Boundary Pressure During Pool Swell, Normalized to Bubble Pressure

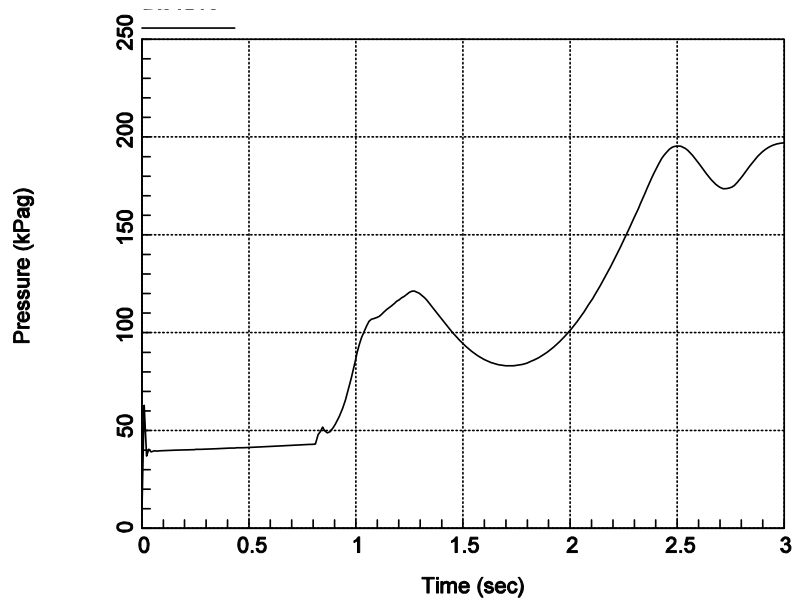
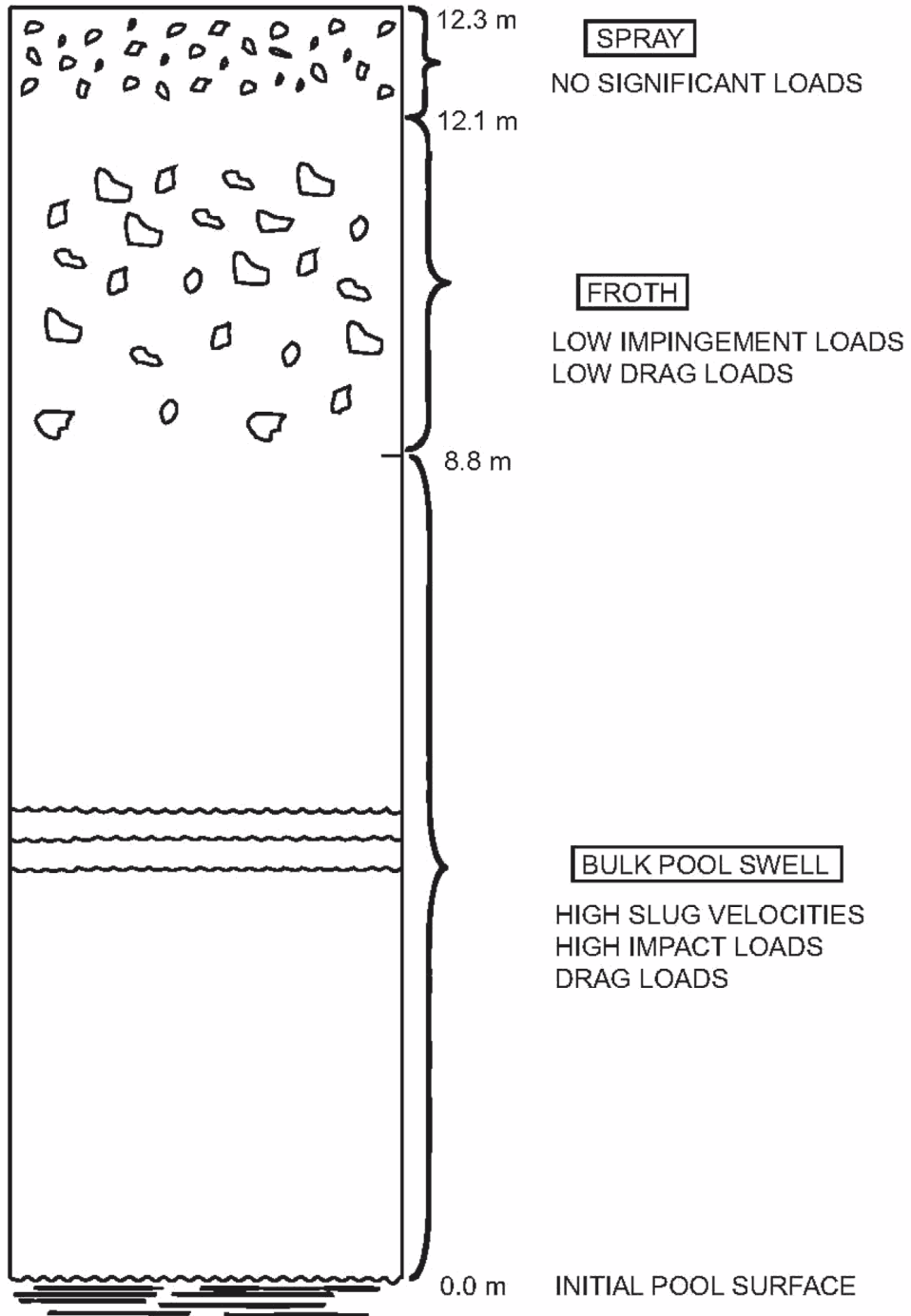


Figure 3B-12 Time History of Air Bubble Pressure



Note: Figure not to scale

Figure 3B-13 Schematic of the Pool Swell Phenomenon

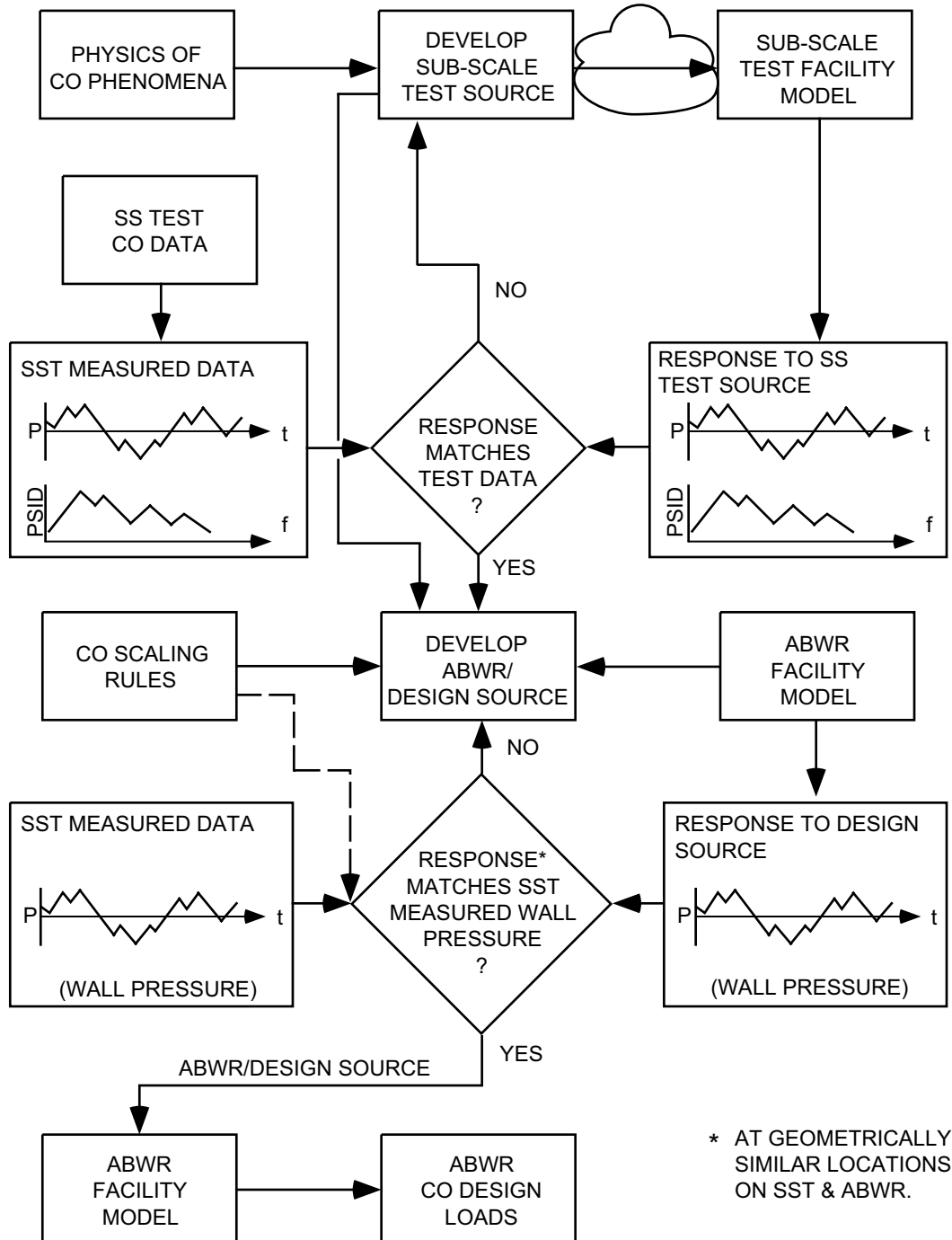


Figure 3B-21 ABWR CO Source Load Methodology

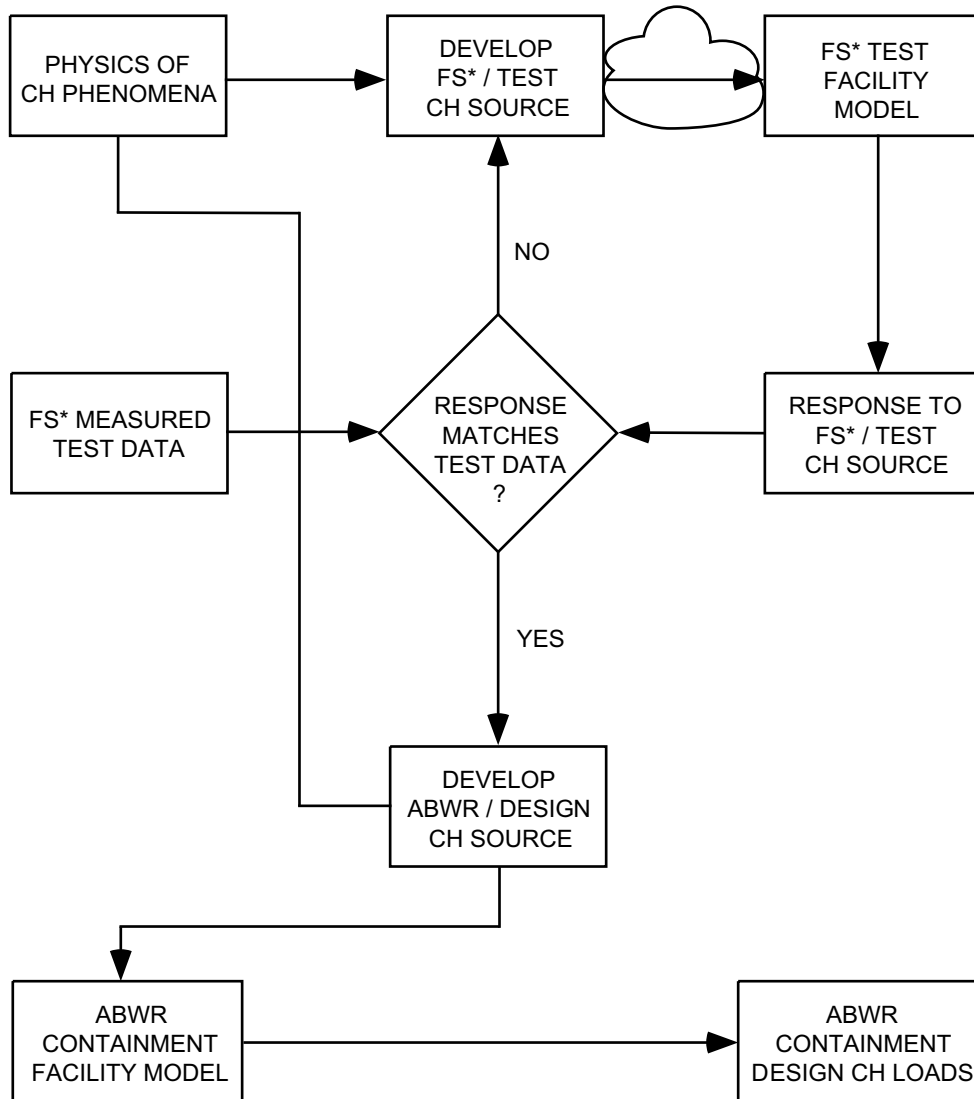


Figure 3B-26 ABWR Chug Source Load Methodology